ORIGINAL PAPER

Nagoya J. Med. Sci. **87**. 22–36, 2025
doi:10.18999/nagjms.87.1.22

Added value of diffusion-weighted magnetic resonance imaging in the diagnosis of recurrent cholangiocarcinoma

Keiichiro Yamada[1], Yasuo Takehara[1,2], Satoko Ishigaki[1], Hiroshi Ogawa[1], Ayumi Nishida[1], Keita Kato[1], Tomoki Ebata[3], Takashi Mizuno[3] and Shinji Naganawa[1]

[1]*Department of Radiology, Nagoya University Graduate School of Medicine, Nagoya, Japan*
[2]*Department of Fundamental Development for Advanced Low Invasive Diagnostic Imaging, Nagoya University Graduate School of Medicine, Nagoya, Japan*
[3]*Department of Surgical Oncology, Nagoya University Graduate School of Medicine, Nagoya, Japan*

ABSTRACT

Distinguishing recurrent cholangiocarcinoma lesions from postoperative fibrosis or biliojejunostomy lesions using contrast-enhanced computed tomography (CECT) alone is challenging. This study examined the value of adding diffusion-weighted magnetic resonance imaging (DWI) to CECT for the detection of cholangiocarcinoma recurrence. This single-institution retrospective analysis included 33 patients who underwent cholangiocarcinoma resection between January 2016 and December 2020. Of the patients, 20 were in the recurrence group and 13 were in the non-recurrence group. Two observers independently reviewed the CECT images and subsequently reviewed the combined CECT and DWI images (b-value, 1000 s/mm^2), with each image reviewed twice. The diagnostic performance was evaluated using receiver operating characteristic (ROC) curve analysis. Kappa statistics were used to evaluate agreement. The diagnostic performance (area under the ROC curve [AUC]) of both observers improved after the addition of DWI; the AUC improved from 0.614 to 0.918 (P = 0.003) in the first session and from 0.820 to 0.928 (P = 0.20) in the second session for Observer A, whereas it improved from 0.566 to 0.858 (P < 0.001) in the first session and from 0.753 to 0.930 (P = 0.02) in the second session for Observer B. The intraobserver and interobserver agreements improved after the addition of DWI; the kappa value improved from 0.586 to 0.656 for Observer A, from 0.371 to 0.838 for Observer B, from 0.308 to 0.766 in the first session, and from 0.464 to 0.620 in the second session. Adding DWI to CECT improves the detection of cholangiocarcinoma recurrence compared to CECT alone.

Keywords: bile ducts, cholangiocarcinoma, magnetic resonance imaging, diffusion-weighted imaging, computed tomography

Abbreviations:
CECT: contrast-enhanced computed tomography
DWI: diffusion-weighted imaging
MRI: magnetic resonance imaging
DR: density ratio
SIR: signal intensity ratio

Received: March 12, 2024; Accepted: June 5, 2024
Corresponding Author: Keiichiro Yamada, MD
Department of Radiology, Nagoya University Graduate School of Medicine,
65 Tsurumai-cho, Showa-ku, Nagoya 466-8550, Japan
Tel: +81-52-744-2327, Fax: +81-52-744-2335, E-mail: ymk.422@icloud.com

AUC: area under the ROC curve

INTRODUCTION

Cholangiocarcinoma is a rare but aggressive cancer of the bile duct epithelium. Surgical resection is the only curative treatment; however, more than half of the lesions recur even after curative resection, and the long-term prognosis is poor.[1] Although chemotherapy or palliative treatment is administered in recurrent settings, recent reports have revealed the superiority of additional surgical resection over chemotherapy in selected patients.[1-4] The indications for secondary resection include solitary and technically resectable disease, satisfactory residual liver volume after the initial surgery, and suitable patient performance status.

Imaging diagnosis plays a vital role in the early detection of "solitary and resectable" recurrent lesions, which may be potentially considered for curative re-resection. Contrast-enhanced computed tomography (CECT) is crucial for such efforts. However, its ability to detect disease relapse remains limited because of the presence of postoperative organ defects, scars (including postoperative fibrosis), and abnormal postoperative anatomical structures (such as biliojejunostomy). Cholangitis, a common postoperative complication, often induces secondary liver abscesses that mimic liver metastasis. ^{18}F-Fluorodeoxyglucose positron emission tomography-computed tomography (PET/CT) is often used to evaluate recurrence. However, it can produce false-negative results for small early stage lesions and false-positive results for liver abscesses. Thus, identifying the most effective imaging modality for early detection of postoperative cholangiocarcinoma recurrence is essential for optimizing patient care after surgery.

Currently, diffusion-weighted imaging (DWI) of the abdomen is widely used. DWI offers additional contrast to magnetic resonance imaging (MRI) by exploiting the Brownian motion of water molecules in tissue. Typically, the intracellular diffusion of water molecules is more restricted than interstitial diffusion. Hence, highly cellular lesions with restricted diffusion exhibit high intensity on DWI and low apparent diffusion coefficients (ADCs).[5,6] Because malignant lesions generally have a higher cell density than benign lesions, DWI can be used to distinguish between them.[7-9] Furthermore, DWI is valuable for detecting lesions because it provides a better contrast between the lesion and surrounding unaffected structures.[10-15] The diagnostic utility of DWI for preoperative detection of cholangiocarcinoma has been reported.[16,17] However, no study has demonstrated the efficacy of DWI for discerning recurrent lesions after surgery for cholangiocarcinoma. The utility of DWI in identifying recurrent lesions has been documented for other malignancies, including head and neck cancer,[18] uterine cervical cancer,[19] pancreatic cancer,[20] and soft tissue tumors.[21]

Therefore, we aimed to examine the value of adding DWI to CECT for detecting recurrent cholangiocarcinoma.

MATERIALS AND METHODS

Study population

Our institutional review board approved this retrospective study (approval No. 2020-0613), and the requirement for informed consent was waived. Instead of a direct informed consent procedure, an opt-out option was made available to potential participants. Details pertaining to this study and the provisions for opting out have been published on the university hospital website.

Table 1 Clinical and pathological data

	Recurrence	Non-recurrence	*P* value
Number of patients	20	13	
Median age (years) [interquartile range]	68.5 [66.0–76.0]	69.0 [66.8–77.3]	0.67
Sex (%)			0.43
Male	70.0 (n = 14)	84.6 (n = 11)	
Female	30.0 (n = 6)	15.4 (n = 2)	
Primary site (%)			0.22
Intrahepatic bile duct	5.0 (n = 1)	23.1 (n = 3)	
Hilar bile duct	80.0 (n = 16)	61.5 (n = 8)	
Distal bile duct	15.0 (n = 3)	15.4 (n = 2)	
Pathological type (%)			0.57
Tubular adenocarcinoma	65.0 (n = 13)	69.2 (n = 9)	
Papillary adenocarcinoma	15.0 (n = 3)	15.4 (n = 2)	
Tubular and papillary adenocarcinoma	10.0 (n = 2)	0 (n = 0)	
Poorly differentiated adenocarcinoma	10.0 (n = 2)	7.7 (n = 1)	
Unknown		7.7 (n = 1)	
Tumor marker			
CEA (ng/mL)	3.23 (1.0–10.6)	3.00 (0.9–5.4)	0.78
CA19-9 (U/mL)	425.0 (7.0–5600)	21.9 (0–44.0)	0.28

Using our database and electronic medical records, we searched for patients who underwent cholangiocarcinoma resection and were monitored for recurrence at our university hospital between January 2016 and December 2020 and identified 418 patients. Cases presenting with intrahepatic, hilar, or distal cholangiocarcinoma as the primary lesion were included. The exclusion criteria were as follows: DWI with a b-value of at least 1000 s/mm^2 was not performed (n = 368); CECT was not performed (n = 4); and the interval between CECT and DWI exceeded 90 days (n = 13). We included 33 patients who underwent CECT and MRI examinations. Among these patients, 20 with recurrent lesions at 24 sites comprised the recurrence group, and the non-recurrence group included 13 patients. The clinical and pathological data of the two groups are summarized in Table 1.

CT protocol

CT was performed using multiple CT systems with 64–320-row detectors; however, the Somatom Definition Flash (Siemens Healthineers, Erlangen, Germany) was primarily used. Other CT systems used were Aquilion One and Aquilion Precision (Canon Medical Systems, Otawara, Japan). Despite the differing imaging conditions, the representative settings were as follows: tube voltage 120 kV; tube current 240–360 mAs; slice thickness 128 × 0.6 mm^2; scan speed 0.33–0.5 s/rotation; and helical pitch 0.5–0.8. CECT was performed using multiple protocols, including equilibrium phase only (n = 18), dynamic two-phase (late arterial phase, portal phase; n = 6), and dynamic five-phase (early arterial phase, late arterial phase, portal phase, equilibrium phase, delayed phase; n = 9). A nonionic contrast agent (Iopamiron 370, Bayer Yakuhin; Omnipaque 300, GE Healthcare Pharma) was injected intravenously. The representative injection speed was 4–5 mL/s, with a 25-mL saline flush at 5 mL/s.

Table 2 Magnetic resonance imaging parameters of diffusion-weighted imaging

	TR (ms)	TE (ms)	b value (s/mm^2)	Slice thickness (mm)	Matrix size	Field of view (cm)	Bandwidth (Hz/pixel)	Noise level
MRI 1	3000	55	0–1000	8	128 × 108	320 × 380	2300	40
MRI 2	3000	50	0–1000	6	128 × 96	262 × 350	2055	40
MRI 3	3400	72	0–1000	6	128 × 82	262 × 350	1953	40
MRI 4	5000	80	0–1000	6	128 × 144	320 × 360	2604	40
MRI 5	4490	73	50–1000	8	148 × 112	302 × 400	2111	40
MRI 6	1800	80	50–1000	6	148 ×108	291 × 400	1535	40

MRI 1, 3T-Skyra; MRI2, 3T-Prisma; MRI 3, 3T-Verio, MRI 4, 3T-Centurion, MRI 5, 1.5T-Avant; MRI 6, 1.5T-Aera.
TR: repetition time
TE: echo time

Table 3 Magnetic resonance imaging parameters of T2-weighted imaging

	TR (ms)	TE (ms)	Slice thickness (mm)	Flip angle	Matrix size	Field of view (cm)	Bandwidth (Hz/pixel)
MRI 1	5000	85	8	120	384 × 187	308 × 379	335
MRI 2	3000	82	6	140	384 × 202	262 × 349	395
MRI 3	4650	91	6	120	384 × 173	262 × 349	334
MRI 4	3400	83	6	-	384 × 256	320 × 360	395
MRI 5	3000	77	8	150	256 × 146	260 × 320	279
MRI 6	3800	79	6	150	256 × 144	262 × 350	280

MRI 1, 3T-Skyra; MRI2, 3T-Prisma; MRI 3, 3T-Verio, MRI 4, 3T-Centurion, MRI 5, 1.5T-Avant; MRI 6, 1.5T-Aera.
TR: repetition time
TE: echo time

MRI protocol

MRI was performed on 1.5T (n = 14) or 3T (n = 19) systems (MAGNETOM Skyra, MAGNETOM Aera, MAGNETOM Prisma, MAGNETOM Avant fit, and MAGNETOM Verio, Siemens Healthineers, Erlangen, Germany; Vantage Centurion, Canon Medical Systems, Otawara, Japan) and a 16- or 18-channel body phased array coil. The protocol included axial T2-weighted imaging (T2WI) and DWI with b-values of 0 or 50 and 1000 s/mm^2. The imaging sequences and parameters are summarized in Tables 2 and 3.

Recurrence

Recurrence was defined as cases with pathological confirmation or cases exhibiting new lesions or lesions with temporal growth within one year detected during retrospective and longitudinal CECT evaluations coupled with strong indications of recurrence based on symptoms, tumor markers, or PET/CT findings. Newly arising lesions identified as abscesses on blood tests or

CECT, particularly those responding to antibiotics and shrinking or disappearing, were classified as non-recurrent. Patients without recurrence indicators or stable tumor markers (CEA and CA19-9) were considered to have no recurrence.

Image analysis

Diagnostic performance. Two image sets were created by an experienced radiologist (K.Y.) who did not participate in the interpretation sessions. The first, a CECT only set, comprised pre–contrast-enhanced CT and CECT images. When a dynamic study was available, arterial, portal, and equilibrium phases were observed. The second, a CECT and DWI set, included pre–contrast-enhanced CT and CECT images as well as MRI incorporating DWI (b-value = 1000 s/mm^2), ADC imaging, and T2WI. Two abdominal radiologists (S.I. [Observer A] with 20 years of experience and Y.T. [Observer B] with 40 years of experience) independently reviewed the image sets and were blinded to the patients' clinical information. Each observer reviewed each image set twice, discerned the recurrent lesions, and documented the recurrence types and confidence levels. In the four reading sessions, the images were presented to the observers in different orders. Each reading session was scheduled at a minimum interval of three weeks. The categorization of recurrence types included local recurrence at the billiojejunostomy site or at the margin of

Table 4 Recurrence types and imaging definition

Recurrence type	Imaging definition
Local recurrence at the billiojejunostomy or the margin of hepatectomy	Irregular soft tissue density with contrast enhancement on CECT Higher intensity on DWI, and lower ADC than the hepatic parenchyma at the site of biliojejunostomy or edge of hepatectomy with or without upstream bile duct dilatation with or without portal vein stenosis
Recurrence or multicentric occurrence in the biliary tree	Non-locoregional intraductal bile duct lesions with contrast enhancement on CECT Higher intensity on DWI, and lower ADCs than the background hepatic or pancreatic parenchyma with or without upstream bile duct dilatation with or without portal vein stenosis
Liver metastasis	Hepatic masses with different contrast enhancement compared to the liver parenchyma on CECT Higher intensity on DWI, and lower ADCs than the hepatic parenchyma Lesions suspicious of AP shunts or hemangioma was categorized as level 2, and alleged abscess was categorized as level 3
Lymph node metastasis	Enlarged lymph nodes with a short diameter of at least 1 cm
Peritoneal dissemination	Peritoneal nodules or lesions with irregular soft tissue density with contrast enhancement on CECT, higher intensity on DWI, and lower ADC than the hepatic parenchyma

CECT: contrast-enhanced computed tomography
DWI: diffusion-weighted imaging
ADC: apparent diffusion coefficient
AP shunt: arterial-portal shunt

the hepatectomy, recurrence or multicentric occurrence in the biliary tree, liver metastasis, lymph node metastasis, and peritoneal dissemination. The confidence level of recurrence was recorded on a five-point scale (1 = no lesion, 2 = a lesion that is unlikely to be tumorous, 3 = possible recurrence, 4 = suspected recurrence, 5 = strongly suspected recurrence). The recurrence types and imaging definitions of the recurrent lesions are listed in Table 4.

The contrast ratio between CT and DWI. With knowledge of the location of the recurrent lesions, the density and signal intensity of the lesions and background unaffected tissues were measured on CECT and DWI. An experienced radiologist (K.Y.) placed the largest possible region of interest (ROI) on a solid or homogeneous portion of the recurrent lesion. The largest lesion was observed when multiple recurrent lesions were present. The ROI area for the lesions ranged from 19 mm^2 to 470 mm^2 (median size, 68 mm^2). The ROI for the background unaffected tissues adjacent to the recurrent lesions, such as hepatic, pancreatic, or fat tissue, were also measured, with the largest possible ROI ranging between 47 mm^2 and 3600 mm^2 (median size 235 mm^2). The contrast ratios, ie, the density ratio (DR) on CECT and the signal intensity ratio (SIR) on DWI, of the recurrent lesions relative to the background unaffected structures were calculated using the following formulas:

SIR = |[(mean lesion signal)-(mean background signal)]/(mean background signal)|,

DR = |[(mean lesion density)-(mean background density)]/(mean background density)|.

(In the above formulas, "| |" denotes absolute value.)

Statistical analyses

Regarding patient demographics, univariable and multivariate analyses were performed to compare the data between the recurrence and non-recurrence groups. Two-tailed t-test or χ^2 test was used in the univariable analysis, and multiple logistic regression analysis was used in the multivariate analysis.

The diagnostic performance of each observer was evaluated using receiver operating characteristic (ROC) curve analysis, and the area under the ROC curve (AUC) was calculated. Pairwise comparisons of the ROC curves were performed to compare the diagnostic performance before and after the addition of DWI. Moreover, the ROC curves for the two reading sessions were compared to evaluate learning effects. The accuracy, sensitivity, specificity, positive predictive value (PPV), and negative predictive value (NPV) for detecting cholangiocarcinoma recurrence were evaluated with 95% confidence intervals for both sessions by each observer based on the assumption of a confidence level of 4 or 5 as a predictor of recurrence. McNemar's test was used to compare the sensitivity and specificity between the interpretation of CECT images alone and between the interpretation of CECT images with DWI. $P < 0.05$ denoted statistical significance. Kappa statistics were used to evaluate the intraobserver and interobserver agreements concerning the correct diagnosis of recurrence. Kappa values <0.20, 0.21–0.40, 0.41–0.60, 0.61–0.80, and >0.80 indicated poor, fair, moderate, good, and excellent agreement, respectively.[22] The DR and SIR were compared using the Wilcoxon signed-rank test. All statistical analyses were performed using Statflex version 7 (Artec, Osaka, Japan).

RESULTS

Study population

A total of 33 patients (25 men and eight women; median age 69 years, interquartile range 66.8–76.3) were included. Multivariate analysis showed that CA19-9 levels ($P = 0.02$) differed significantly between the recurrence and non-recurrence groups. The distribution of recurrence

locations in this study was as follows: 40% recurrence at the biliojejunostomy or the edge of the hepatectomy site (Fig. 1, Fig. 2); 15% recurrence or multicentric occurrence in the biliary tree (Fig. 1); 45% liver metastasis; 10% lymph node metastasis (5% solitary, 5% multiple); and 10% peritoneal dissemination (Table 5).

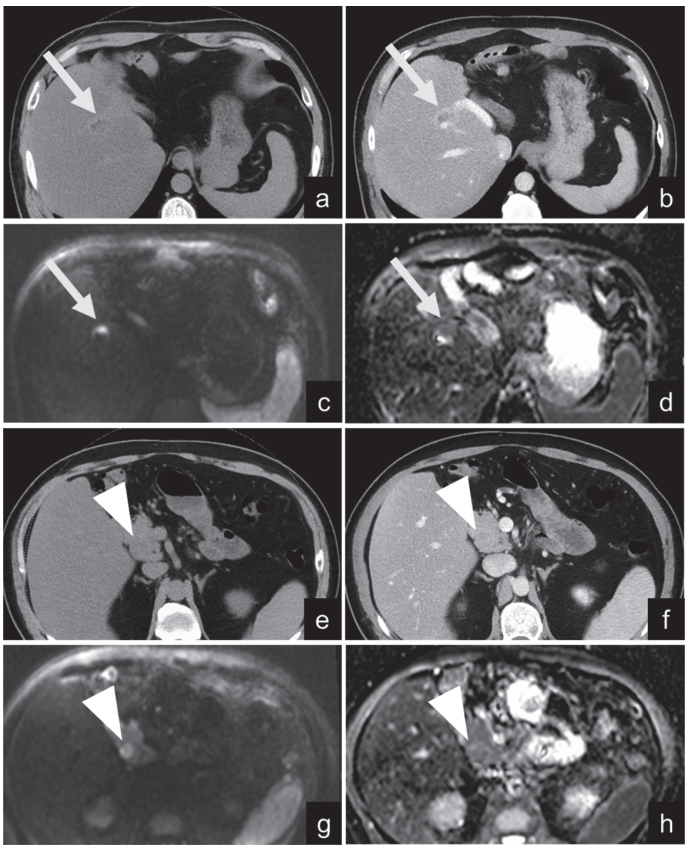

Fig. 1 CT and MRI in a 52-year-old man with recurrence at the site of biliojejunostomy and intrapancreatic bile duct four years after surgery for hilar cholangiocarcinoma

The recurrent lesion at the biliojejunostomy site (arrows) displays isoattenuation at the surrounding hepatic parenchyma on pre-contrast CT (a) and CECT (b). The lesion exhibits hyperintensity on DWI (c) and isointensity on ADC imaging (b-value = 1000 s/mm^2) (d) compared with the surrounding hepatic parenchyma. The recurrent lesion in the intrapancreatic bile duct (arrowheads) shows the same attenuation as the surrounding pancreatic parenchyma on pre-contrast CT (e) and CECT (f). The lesion exhibits hyperintensity on DWI (g) and hypointensity on ADC imaging (h) relative to the surrounding pancreatic parenchyma.

ADC: apparent diffusion coefficient
CECT: contrast-enhanced CT
CT: computed tomography
DWI: diffusion-weighted imaging
MRI: magnetic resonance imaging

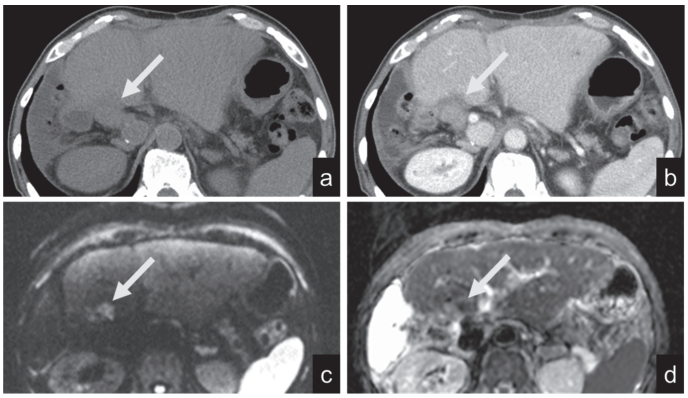

Fig. 2 CT and MRI in a 71-year-old man with recurrence at the site of biliojejunostomy nine months after surgery for hilar cholangiocarcinoma

The recurrent lesion (arrows) shows low attenuation compared to the surrounding hepatic parenchyma or jejunum on pre-contrast CT (a) and CECT (b). The lesion exhibits hyperintensity on DWI (b-value = 1000 s/mm^2) (c) and hypointensity on ADC imaging (d) relative to the surrounding hepatic parenchyma or jejunum.
ADC: apparent diffusion coefficient
CECT: contrast-enhanced CT
CT: computed tomography
DWI: diffusion-weighted imaging
MRI: magnetic resonance imaging

Table 5 Distribution of recurrence locations

Recurrence locations	**%**
Biliojejunostomy or the edge of hepatectomy	40.0 (n = 8)
Recurrence or multicentric occurrence in the biliary tree	15.0 (n = 3)
Intrapancreatic bile duct	10.0 (n = 2)
Hilar bile duct	5.0 (n = 1)
Liver metastasis	45.0 (n = 9)
Solitary	20.0 (n = 4)
Multiple	25.0 (n = 5)
Lymph node metastasis	10.0 (n = 2)
Solitary	5.0 (n = 1)
Multiple	5.0 (n = 1)
Peritoneal dissemination	10.0 (n = 2)

Diagnostic performance

The comparison data of the diagnostic efficacy of CECT alone, as opposed to the combined modality of CECT and DWI, are summarized in Table 6. A pivotal observation was the substantial enhancement in the AUC for diagnosing recurrent cholangiocarcinoma with the addition of DWI in the first session by Observer A (0.614 vs 0.918, $P = 0.003$) and in both sessions by Observer B (first session: 0.566 vs 0.858, $P < 0.001$; second session: 0.753 vs 0.930, $P = 0.02$). While the second session of Observer A did not demonstrate statistically significant augmentation, it is important to note that there was still an increase in the AUC (from 0.820 to 0.928, $P = 0.20$; Fig. 3).

Table 6 Comparison of the diagnostic performance of CECT alone and CECT/DWI for evaluating cholangiocarcinoma recurrence

		Observer A			Observer B		
		1st	2nd	*P* value[a)]	1st	2nd	*P* value[a)]
CECT alone	AUC	0.614	0.820	0.005*	0.566	0.753	0.03*
	Accuracy (%)	51.4	64.9		51.4	59.5	
	Sensitivity (%)	33.3	54.2		45.8	41.7	
	Specificity (%)	84.6	84.6		61.5	92.3	
	PPV (%)	80.0	86.7		68.8	90.9	
	NPV (%)	40.7	50.0		38.1	46.2	
CECT and DWI	AUC	0.918	0.928	0.77	0.858	0.930	0.28
	Accuracy (%)	89.1	83.8		83.8	86.5	
	Sensitivity (%)	91.7	83.3		79.2	79.2	
	Specificity (%)	84.6	84.6		100	100	
	PPV (%)	91.7	90.9		100	100	
	NPV (%)	84.6	73.3		68.4	72.2	
***P* value[b)]**		0.003*	0.20		<0.001*	0.02*	
***P* calculated using the McNemar test**							
	Sensitivity	< 0.001*	< 0.001*		0.01*	< 0.001*	
	Specificity	0.63	0.50		< 0.001*	< 0.001*	

CECT: contrast-enhanced computed tomography
DWI: diffusion-weighted imaging
AUC: area under the ROC curve
ROC: receiver operating characteristic
PPV: positive predictive value
NPV: negative predictive value
[a)] *P* value for comparison of the AUC between the two sessions
[b)] *P* value for comparison of the AUC between CECT alone and CECT with DWI
* statistical significance ($P < 0.05$)

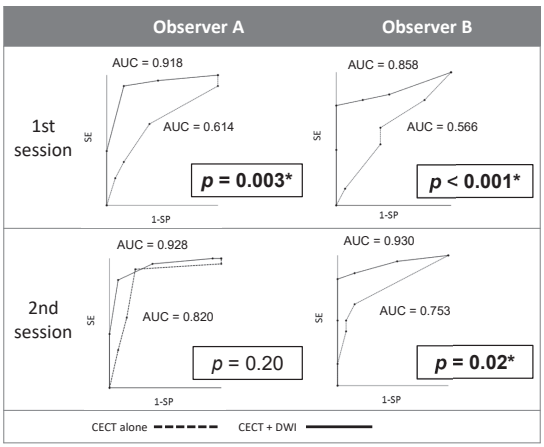

Fig. 3 The AUC of receiver operating characteristic analysis
The AUC improved from 0.614 to 0.918 ($P = 0.003$) in the first session and from 0.820 to 0.928 ($P = 0.20$) in the second session for Observer A, and from 0.566 to 0.858 ($P < 0.001$) in the first session and from 0.753 to 0.930 ($P = 0.02$) in the second session for Observer B.
AUC: area under the curve
* statistical significance ($P < 0.05$)

Table 7 Intraobserver agreement of confidence levels between the first and second sessions

	CECT alone	CECT and DWI
Kappa for Observer A	0.586	0.656
Kappa for Observer B	0.371	0.838

CECT: contrast-enhanced computed tomography
DWI: diffusion-weighted imaging

Table 8 Interobserver agreement of confidence levels between Observers A and B

	CECT alone	CECT and DWI
Kappa for the first session	0.308	0.766
Kappa for the second session	0.464	0.620

CECT: contrast-enhanced computed tomography
DWI: diffusion-weighted imaging

Furthermore, when using CECT alone, both observers exhibited enhanced diagnostic performance in the second session compared to the first session (Observer A: AUC 0.614 vs 0.820, $P = 0.005$; Observer B: AUC 0.566 vs 0.753, $P = 0.03$).

In terms of sensitivity and specificity, Observer B showed significant improvements after integrating DWI with CECT (first session sensitivity: 45.8% vs 79.2%, $P = 0.01$; specificity: 61.5% vs 100%, $P < 0.001$; second session sensitivity: 41.7% vs 79.2%, $P < 0.001$; specificity: 92.3% vs 100%, $P < 0.001$). Similarly, Observer A exhibited improvements in sensitivity (first session: 33.3% vs 91.7%, $P < 0.001$; second session: 54.2% vs 83.3%, $P < 0.001$), with no significant change in specificity (first session: 84.6% vs 84.6%, $P = 0.63$; second session: 84.6% vs 84.6%, $P = 0.50$).

The incorporation of DWI demonstrated an enhancement in PPV for Observer A (first session: from 80.0 to 91.7%; second session: from 86.7% to 90.9%) and Observer B (first session: from 68.8% to 100%; second session: from 90.9% to 100%) and NPV for Observer A (first session: from 40.7 to 84.6%; second session: from 50.0% to 73.3%) and Observer B (first session: from 38.1% to 68.4%; second session: from 46.2% to 72.2%).

Intraobserver agreement improved with the addition of DWI. Specifically, the kappa value improved from 0.586 (moderate) to 0.656 (good) for Observer A and from 0.371 (fair) to 0.838 (excellent) for Observer B (Table 7). In addition, interobserver agreement also improved after the addition of DWI in the first session (from 0.308 [fair] to 0.766 [good]) and the second session (from 0.464 [moderate] to 0.620 [good]) (Table 8).

Contrast ratio between CT and DWI

The SIR on DWI (median 0.847; interquartile range 0.405–1.657) was significantly higher than the DR on CECT (median 0.332; interquartile range 0.233–0.482) ($P < 0.001$; Fig. 4).

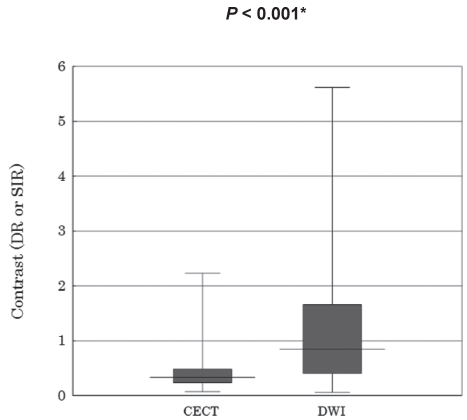

Fig. 4 Comparison of the DR on CECT and SIR on DWI
The SIR on DWI (median, 0.847; interquartile range, 0.405–1.657) was significantly higher than the DR on CECT (median, 0.332; interquartile range, 0.233–0.482) ($P < 0.001$).
CECT: contrast-enhanced computed tomography
DR: density ratio
DWI: diffusion-weighted imaging
SIR: signal intensity ratio
* statistical significance ($P < 0.05$)

DISCUSSION

Adding DWI to CECT improved the diagnostic performance for evaluating cholangiocarcinoma recurrence in two independent observers with over 20 years of experience in abdominal radiology. For instance, addition of DWI achieved higher AUC and sensitivity for detecting recurrent lesions. Although not statistically significant, the AUC improved in the second session for Observer A. This augmentation implies a trend toward enhanced diagnostic performance with the inclusion of DWI with CECT. PPV and NPV also improved after the addition of DWI to CECT. Moreover, the addition of DWI increased the intraobserver and interobserver agreements.

In the second session of Observer A, the enhancement in the AUC with the incorporation of DWI did not reach statistical significance. This outcome could be attributed to the heightened specificity noted during Observer A's second session, even with CECT alone, which potentially augmented Observer A's interpretive acumen and expertise. Conversely, measures such as accuracy, sensitivity, PPV, and NPV, in addition to AUC and specificity, all exhibited enhancement, indicative of the overall improvement in diagnostic performance facilitated by the inclusion of DWI.

For both observers, diagnostic performance was higher in the second session than in the first session for each imaging set using CECT alone. These results may be attributed to the learning curve for detecting cholangiocarcinoma recurrence, which was particularly substantial with CECT alone. Even experienced readers can miss recurrent lesions in their first reading of CECT images. However, after adding DWI, the diagnostic performance did not improve between the first and second sessions, presumably because the recurrent lesions were easily identified on DWI. In fact, the SIR on DWI was substantially higher than the DR on CECT in the semi-quantitative evaluation, indicating that the contrast between the recurrent lesion and surrounding structures was more distinct on DWI. These findings suggest the impact of adding DWI to the evaluation of cholangiocarcinoma recurrence.

Among the several types of disease recurrence, recurrence at the residual intrapancreatic

bile duct shows a specific clinical feature in which the foci are often resected by secondary pancreaticoduodenectomy with curative intent.[23,24] Therefore, this type of recurrence should be appropriately diagnosed, although it is typically not considered in standard postoperative patient care. Indeed, in some patients, intrapancreatic bile duct recurrence is difficult to detect using CECT alone for two major reasons. First, because previous hepatobiliary resection discontinued the intrapancreatic duct, there were no clinical signs of upstream biliary dilatation. Second, CECT exhibited the same attenuation between the recurrent foci and pancreatic parenchyma, masking their presence. It remains controversial whether recurrent lesions of the intrapancreatic bile duct are treated as metastases from the initial cholangiocarcinoma or metachronous multicentric tumor growth because the intrapancreatic bile duct was extensively surveyed prior to the initial surgery, confirming it was naïve. Such multicentricity is a typical feature of intraductal papillary neoplasms of the bile duct (IPNB).[25-28] DWI is particularly advantageous for highlighting IPNB because these tumors exhibit extremely high intensity on DWI owing to their high cellularity.[29] Conversely, the diagnostic efficacy of DWI remained consistent in detecting recurrence despite the prevalence of tubular adenocarcinoma in the patient cohort. This implies that the inclusion of DWI confers a discernible supplementary benefit, irrespective of the histological subtype.

Concerning imaging-based evaluation of recurrent lesions, Corvera et al[30] found that PET/CT had high sensitivity and specificity for identifying cholangiocarcinoma recurrence (89% and 100%, respectively; n = 33). However, recurrence had already identified on cross-sectional imaging in almost all patients in that study. Thus, the diagnostic performance of the initial evaluation of recurrent lesions remains unclear. Zhuo et al[31] reported that nonperipheral high signal intensity on DWI is useful for distinguishing liver abscesses from liver metastases of various tumors. In our study, one patient had a liver abscess; however, both observers suspected metastasis on CECT alone. Indeed, nonperipheral high signal intensity was observed on DWI, and both observers revised the diagnosis to liver abscess after adding DWI. Satoh et al[32] noted that DWI ranked second after PET/CT in terms of the diagnostic yield of peritoneal dissemination. In the context of our study, we encountered two instances of peritoneal dissemination. In one example, DWI revealed a disseminated lesion that was not detected by CECT alone, thereby permitting an accurate diagnosis.

In a previous study on other malignancies, DWI was used for primary lesion identification. However, our study was focused on the detection of "recurrent lesions" in cholangiocarcinoma. In cases of recurrence, the presence of postoperative organ deficits necessitates more stringent resectability criteria, making early detection imperative for therapeutic efficacy. Based on the findings of our study, the amalgamation of CECT and DWI is proposed to enhance the detection efficacy of early lesions amenable to therapeutic resections. Furthermore, while previous studies have documented local recurrence after pancreatic cancer surgery, our study posits that DWI may enhance diagnostic performance for various forms of recurrence beyond local manifestations.

Although the addition of DWI increases time and cost expenditures, its unique advantage lies in its potential to extend patient survival and maximize the efficiency of expensive chemotherapy by facilitating the early detection of recurrent lesions, thereby justifying the investment. Notably, some patients in the recurrence group achieved cancer-free and long-term survival with subsequent resection of the recurrent lesions. Future studies employing CECT with DWI may reveal its utility and cost-effectiveness.

In practical clinical settings, MRI requires a longer examination time than CT and is accessible with fewer devices, thereby reducing the number of feasible examinations. Hence, to incorporate MRI into periodic follow-ups, the examination time must be abbreviated. Additionally, reducing examination costs and minimizing patient invasiveness are crucial for routine assessments. This study is noteworthy for restricting the MRI sequences to DWI and T2WI, yet it remarkably

enhanced the diagnostic performance for cholangiocarcinoma recurrence. These findings suggest a significant enhancement in recurrence diagnosis, even with fewer ancillary tests, thereby minimizing examination time, costs, and patient invasiveness. Contrast-enhanced MRI was not evaluated in this study. This decision stems from our belief that lesion contrast effects can be adequately determined using routine follow-up CECT. From our perspective, the use of contrast agents for MRI raises concerns associated with extended examination times, unnecessary patient invasiveness, and inefficient use of medical resources. In addition to DWI and T2WI, the inclusion of T1-weighted images and magnetic resonance cholangiopancreatography (MRCP), as warranted by the examination time, is advised to evaluate anatomical morphology and intrahepatic biliary stones.[33] Typically, postoperative surveillance after cholangiocarcinoma surgery is conducted every three to six months for approximately ten years. In addition to CECT, it is advisable to include annual MRI scans featuring DWI, T2WI, T1WI, and MRCP. Gadolinium ethoxybenzyl-diethylenetriaminepentaacetic acid-enhanced MRI (EOB-MRI) should be performed when liver metastases are suspected. Further studies are required to determine the optimal combination of sequences for comprehensive follow-up evaluation.

This study has a few limitations. First, this was a single-center, retrospective study with a relatively small sample size. Second, the sample size was small because regular MRI follow-ups are not scheduled after cholangiocarcinoma surgery in the current clinical protocol; therefore, many cases were excluded. Third, some patients who underwent MRI after recurrence were diagnosed through other examinations, which may have caused a selection bias. Fourth, CECT was performed using various contrast protocols, and MRI was performed using multiple parameters, and this difference in imaging methods could have influenced the results.

In conclusion, the addition of DWI to CECT significantly improved the diagnostic performance for detecting recurrent cholangiocarcinoma. These results highlight the potential role of DWI, in addition to CECT, in surveillance after cholangiocarcinoma resection.

ACKNOWLEDGMENT

We are indebted to Yoshinori Tsutsumi and Minako Kawamura for technical assistances. We would like to thank Editage (www.editage.jp) for English language editing.

CONFLICTS OF INTEREST

Yasuo Takehara is a faculty member of the Nagoya University, Department of Fundamental Development for Advanced Low Invasive Diagnostic Imaging, which is endowed by a private company, HIMEDIC, Inc. The other authors have no relevant financial or non-financial interests to disclose.

REFERENCES

1 Takahashi Y, Ebata T, Yokoyama Y, et al. Surgery for Recurrent Biliary Tract Cancer: A Single-center Experience with 74 Consecutive Resections. *Ann Surg*. 2015;262(1):121–129. doi:10.1097/SLA.0000000000000827
2 Lang H. Surgical Approach to Recurrent Cholangiocarcinoma. *Visc Med*. 2021;37(1):26–31. doi:10.1159/000513711
3 Tokuda K, Morine Y, Saito Y, et al. Effectiveness of repeat surgery for recurrence after primary hepatectomy in patients with intrahepatic cholangiocarcinoma. *Int J Clin Oncol*. 2020;25(12):2083–2089. doi:10.1007/s10147-020-01775-x
4 Maki H, Kawaguchi Y, Nagata R, et al. Conditional recurrence analysis of intrahepatic cholangiocarcinoma:

Changes in recurrence rate and survival after recurrence resection by disease-free interval. *Hepatol Res*. 2023;53(12):1224–1234. doi:10.1111/hepr.13951
5 Koh DM, Collins DJ. Diffusion-weighted MRI in the body: applications and challenges in oncology. *AJR Am J Roentgenol*. 2007;188(6):1622–1635. doi:10.2214/AJR.06.1403
6 Bonekamp S, Corona-Villalobos CP, Kamel IR. Oncologic applications of diffusion-weighted MRI in the body. *J Magn Reson Imaging*. 2012;35(2):257–279. doi:10.1002/jmri.22786
7 Guo Y, Cai YQ, Cai ZL, et al. Differentiation of clinically benign and malignant breast lesions using diffusion-weighted imaging. *J Magn Reson Imaging*. 2002;16(2):172–178. doi:10.1002/jmri.10140
8 Miller FH, Hammond N, Siddiqi AJ, et al. Utility of diffusion-weighted MRI in distinguishing benign and malignant hepatic lesions. *J Magn Reson Imaging*. 2010;32(1):138–147. doi:10.1002/jmri.22235
9 Fujii S, Kakite S, Nishihara K, et al. Diagnostic accuracy of diffusion-weighted imaging in differentiating benign from malignant ovarian lesions. *J Magn Reson Imaging*. 2008;28(5):1149–1156. doi:10.1002/jmri.21575
10 Takakura K, Sumiyama K, Munakata K, et al. Clinical usefulness of diffusion-weighted MR imaging for detection of pancreatic cancer: comparison with enhanced multidetector-row CT. *Abdom Imaging*. 2011;36(4):457–462. doi:10.1007/s00261-011-9728-7
11 Tsai TH, Hsu JS, Lai ML, Liu GC, Shih MC, Chen CY. Added value of diffusion-weighted imaging to MR cholangiopancreatography for the diagnosis of bile duct dilatations. *Abdom Radiol (NY)*. 2016;41(3):485–492. doi:10.1007/s00261-015-0612-8
12 Jang KM, Kim SH, Lee SJ, Park HJ, Choi D, Hwang J. Added value of diffusion-weighted MR imaging in the diagnosis of ampullary carcinoma. *Radiology*. 2013;266(2):491–501. doi:10.1148/radiol.12121106
13 Shinya S, Sasaki T, Nakagawa Y, Guiquing Z, Yamamoto F, Yamashita Y. The usefulness of diffusion-weighted imaging (DWI) for the detection of gastric cancer. *Hepatogastroenterology*. 2007;54(77):1378–1381.
14 Takahara T, Imai Y, Yamashita T, Yasuda S, Nasu S, Van Cauteren M. Diffusion weighted whole body imaging with background body signal suppression (DWIBS): technical improvement using free breathing, STIR and high resolution 3D display. *Radiat Med*. 2004;22(4):275–282.
15 Kwee TC, Takahara T, Ochiai R, Nievelstein RA, Luijten PR. Diffusion-weighted whole-body imaging with background body signal suppression (DWIBS): features and potential applications in oncology. *Eur Radiol*. 2008;18(9):1937–1952. doi:10.1007/s00330-008-0968-z
16 Cui XY, Chen HW, Cai S, et al. Diffusion-weighted MR imaging for detection of extrahepatic cholangiocarcinoma. *Eur J Radiol*. 2012;81(11):2961–2965. doi:10.1016/j.ejrad.2011.12.040
17 Yoon HJ, Kim YK, Jang KT, et al. Intraductal papillary neoplasm of the bile ducts: description of MRI and added value of diffusion-weighted MRI. *Abdom Imaging*. 2013;38(5):1082–1090. doi:10.1007/s00261-013-9989-4
18 Kim M, Lee JH, Joo L, et al. Development and Validation of a Model Using Radiomics Features from an Apparent Diffusion Coefficient Map to Diagnose Local Tumor Recurrence in Patients Treated for Head and Neck Squamous Cell Carcinoma. *Korean J Radiol*. 2022;23(11):1078–1088. doi:10.3348/kjr.2022.0299
19 Lucas R, Lopes Dias J, Cunha TM. Added value of diffusion-weighted MRI in detection of cervical cancer recurrence: comparison with morphologic and dynamic contrast-enhanced MRI sequences. *Diagn Interv Radiol*. 2015;21(5):368–375. doi:10.5152/dir.2015.14427
20 Shin N, Kang TW, Min JH, et al. Utility of Diffusion-Weighted MRI for Detection of Locally Recurrent Pancreatic Cancer After Surgical Resection. *AJR Am J Roentgenol*. 2022;219(5):762–773. doi:10.2214/AJR.22.27739
21 Hu P, Zhang S, Zhou Z. The value of bi-exponential and non-Gaussian distribution diffusion-weighted imaging in the differentiation of recurrent soft tissue neoplasms and post-surgical changes. *Ann Transl Med*. 2020;8(21):1357. doi:10.21037/atm-20-2025
22 McHugh ML. Interrater reliability: the kappa statistic. *Biochem Med (Zagreb)*. 2012;22(3):276–282.
23 Shinohara K, Shimoyama Y, Ebata T, et al. Clinicopathologic study on metachronous double cholangiocarcinomas of perihilar and subsequent distal bile duct origin. *Surgery*. 2017;162(1):84–93. doi:10.1016/j.surg.2016.12.034
24 Kwon HJ, Kim SG, Chun JM, Hwang YJ. Classifying extrahepatic bile duct metachronous carcinoma by de novo neoplasia site. *World J Gastroenterol*. 2014;20(11):3050–3055. doi:10.3748/wjg.v20.i11.3050
25 Kageyama Y, Yamaguchi R, Watanabe S, Aizu K, Sato F, Arimoto A. Intraductal papillary neoplasm of the bile duct with rapidly progressive multicentric recurrence: A case report. *Int J Surg Case Rep*. 2018;51:102–106. doi:10.1016/j.ijscr.2018.08.024
26 Narita M, Endo B, Mizumoto Y, et al. Multicentric recurrence of intraductal papillary neoplasms of bile duct in the remnant intrahepatic bile duct after curative resection. *Int J Surg Case Rep*. 2015;12:123–127.

doi:10.1016/j.ijscr.2015.05.033
27 Ito T, Hisa T, Ito Y, et al. Intraductal papillary neoplasm of the bile duct with metachronous development in the downstream bile duct after radical resection. *Clin J Gastroenterol*. 2024;17(1):155–163. doi:10.1007/s12328-023-01867-x
28 Brennan GT, Lee JG. Metachronous Intraductal Papillary Neoplasm of the Bile Duct and Intraductal Papillary Mucinous Neoplasm of the Pancreas in a Patient Diagnosed with Mucinous Adenocarcinoma. *ACG Case Rep J*. 2019;6(2):e00023. doi:10.14309/crj.0000000000000023
29 Stendahl K, Gilani SM, Basturk O, Hui P, Sigel C, Cai G. Intraductal papillary neoplasm of the bile duct: Cytomorphologic and molecular features. *Cancer Cytopathol*. 2023;131(1):37–49. doi:10.1002/cncy.22637
30 Corvera CU, Blumgart LH, Akhurst T, et al. 18F-fluorodeoxyglucose positron emission tomography influences management decisions in patients with biliary cancer. *J Am Coll Surg*. 2008;206(1):57–65. doi:10.1016/j.jamcollsurg.2007.07.002
31 Zhuo LY, Xing LH, Ma X, et al. Differentiating Between an Atypical Hepatic Abscess and Tumor Metastasis Using Magnetic Resonance Imaging and Hepatobiliary Phase Imaging. *Infect Drug Resist*. 2021;14:3263–3274. doi:10.2147/IDR.S318291
32 Satoh Y, Ichikawa T, Motosugi U, et al. Diagnosis of peritoneal dissemination: comparison of 18F-FDG PET/CT, diffusion-weighted MRI, and contrast-enhanced MDCT. *AJR Am J Roentgenol*. 2011;196(2):447–453. doi:10.2214/AJR.10.4687
33 Kim YK, Kim CS, Lee JM, et al. Value of adding T1-weighted image to MR cholangiopancreatography for detecting intrahepatic biliary stones. *AJR Am J Roentgenol*. 2006;187(3):W267-W274. doi:10.2214/AJR.05.0266